



Impact of multi-characteristics on heavy metals sensor-based surface plasmonic resonance

Ali Abdulkhaleq Alwahib¹ · Shatha Mezher Hasan²

Received: 24 July 2023 / Accepted: 27 September 2023 / Published online: 24 October 2023
© The Author(s), under exclusive licence to The Optical Society of India 2023

Abstract A fiber-based surface plasmon resonance (SPR) sensor is investigated in this study. Initially, a D-shaped optical fiber is studied under different types and brands of light sources, optical spectrometers, and polarizing angles. The best stability with low noise is a supercontinuum light source with Avantes spectrometer. Using the polarizer controller to tune the width and dip shows the minimum absorption point when waveplates are set at 90°, 0°, and 45°. The temperature effects are recognized as shifts in absorption ranging from 30 to 60 °C for fiber-based SPR (with and without a polarizer controller). In the photoelastic effect, the sensor shows significant variation according to the applied load, with a maximum sensitivity of 1.05 nm/g at 5 g weight. Stability, response time, and selectivity are also discussed. Results are used to analyze the plasmonic sensor efficiency for Hg ions detection. It appears that there is a lack of information regarding the light types and polarization angles within a D-shaped fiber for Hg ions SPR sensor. As of now, there seems to be no published literature that has thoroughly explored this topic under different conditions.

Keywords Sensor · Optical fiber · Polarizer · Heavy metals · Plasmonic

Introduction

The excitation principle of SPR depends on the coupling condition between the incident light wave and SP (i.e., an optical wave interacting with SP). When the plasmon wave interacts with analytcs, a phase shift, intensity shift, and spectral transmission shift in optical signal may occur. According to this interaction, fiber-based SPR sensors are classified as (1) wavelength modulation, (2) intensity modulation, and (3) phase modulation [1, 2].

In the wavelength modulation method, the dip position of the maximum absorption wavelength of the incident light is always measured [3]. This spectral shift is associated with the refractive index of the analyte solution or sensing layer. The refractive index and thickness could change the intensity modulation of SPR (i.e., the optical length) in the dielectric layer [4]. In the phase modulation method, the phase shift is calculated at a single angle and wavelength of the incident light wave and applied as an output for different applications [5]. The temperature substantially affects the plasmonic waves because their accuracy decreases and induces cross-interference [6]. However, the temperature effect can become efficient in applications using the phase change monitoring technique [7]. In this type of physics parameter (temperature), 120 °C is the maximum limit to preserve effective plasmonic waves [8]. Another physical property is a light source for exciting SP, which is still an obstacle to developing the SPR-based sensor [9]. Laser or halogen lamps are bulky light sources used in excitation SPR-based sensor applications. An inorganic source such as light-emitting diodes replaced these lights. The making of an inorganic light source stands in need of an epitaxial technique and crystalline substrate, which is a considerable drawback of these changes. Therefore, components and molding steps must be consolidated with the SPR sensor design [9]. Foster,

✉ Ali Abdulkhaleq Alwahib
Ali.A.Alwahib@uotechnology.edu.iq

¹ Department of Laser and Optoelectronics Engineering,
University of Technology-Iraq, Baghdad, Iraq

² Iraqi commission for computers and informatics, Informatic
institute for postgraduate studies, Baghdad, Iraq

supported by co-researchers, excited SPs using a convergent light beam from a monochromatic light source [10]. Different light sources were applied to excite SP, such as broadband light sources with an 840 nm center wavelength [11]; for prism-based SPR, a white light source (halogen lamp) is used [12]. Broadband and a single wavelength were applied. Au layers are applied to a semiconductor laser (GaAs) light source to excite PSs at $\lambda = 650$ nm. A polarizer supports some light sources to excite SPs. Researchers adapted different light sources, but no clear reasons were provided for applying this type. However, one critical factor is system noise, namely the fluctuation of the light source and temperature effect (index change) [13]. An organic light-emitting diode was used to excite the SP phenomenon, and this type of light source does not require coupling the light source from external into the sensor design. This light source has peak wavelengths of 625, 530, and 465 nm [9]. The light parameters are connected directly to the polarization measurements because of polarization type s or p-polarization on the excitation of plasmonic waves [14].

The polarization angle influences the dip of the plasmonic resonance absorption and, thus, the transmission. The behavior of the transmission dip spectrum according to the polarization states of the input light beam can be studied using a free space polarization controller with three rotating waveplates [15].

The present work investigates and characterizes plasmonic waves based on wavelength and intensity modulation under different physical properties. The light types and polarization angles within a D-shaped fiber for Hg ions SPR sensor have not yet been thoroughly explored, nor has it been published under other conditions in any literature thus far.

Experimental setup

For the SPR evaluation, a multimode D-shaped optical fiber with a 62.5 μm core diameter and a 125 μm cladding diameter was used. This optical fiber was acquired from Phoenix Photonics Ltd., which uses an in-house grinding and polishing technique to remove a section of the optical fiber [16]. Evanescent waves can be harnessed for sensing applications by removing the cladding section of an optical fiber. The polished regions' lengths are 17 mm and 25 mm for this

research work, and the insertion loss in the air is less than 0.1 dB [15].

Three main experiments were performed to evaluate the plasmonic behavior. The first experiment used the shorter-length region to achieve better quality parameters [17]. The setup of SPR consists of an MMF D-shaped optical fiber (polished region length is 17 mm), a spectrometer, and a light source, as shown in Fig. 1. A 1-halogen white light serves as the light source, and a 2-A supercontinuum as the laser source. Both light sources were attached to the spectrometer types (Ocean Optics) and spectrometer types (Avantes). The positive evaluation of the results for the first experiment (the light source and spectrometer) is applied to the subsequent experiments.

The second experimental setup for SPR consists of a light source, a polarization controller, a D-shaped fiber (polished regions' lengths are 17 mm and 25 mm), a spectrometer, and a computer equipped with spectroscopy software. The light source covers a bandwidth from 300 nm to 1100 nm. The wavelength range of interest is between 500 nm and 700 nm, coinciding with the Au resonance wavelength [18]. The light from this source is randomly polarized using a polarizer controller. The polarization controller consists of two quarter-waveplates (QWP) and a half-wave plate (HWP) in a sequence of QWP-HWP-QWP, as shown in Fig. 2. The state of light polarization is investigated by varying the half-waveplates and quarter-wave plate given that light polarization influences the SPR.

The third SPR experimental setup was built on the previous experiment. In this experiment, deionized water at a range of temperatures was dropped slowly on the flat area (coated gold layer) to trace the influence of heat. This experiment was applied for prism-based SPR and fiber-based SPR excited using 633 nm laser and wideband light sources, respectively.

The fourth and fifth experiments evaluate the photoelastic effect and the stability performance of the sensor under the effects of the maximum positive results of the measured parameters. The photoelastic effect based on external stresses can cause changes in the state of polarization. The loads applied are 10 and 15 g and then compared with zero load. However, the stability is achieved using Hg²⁺ ion solution. The transmission spectrum is recorded by measuring the output directly from the light source throughout the D-shaped optical fiber.

Fig. 1 Light source variation of SPR setup

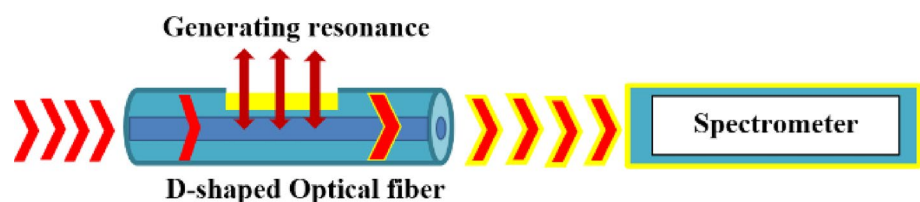


Fig. 2 D-shaped optical fiber polarization for setup

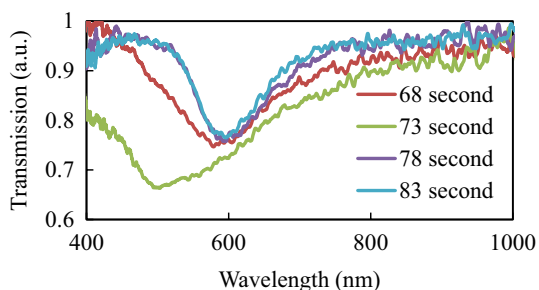
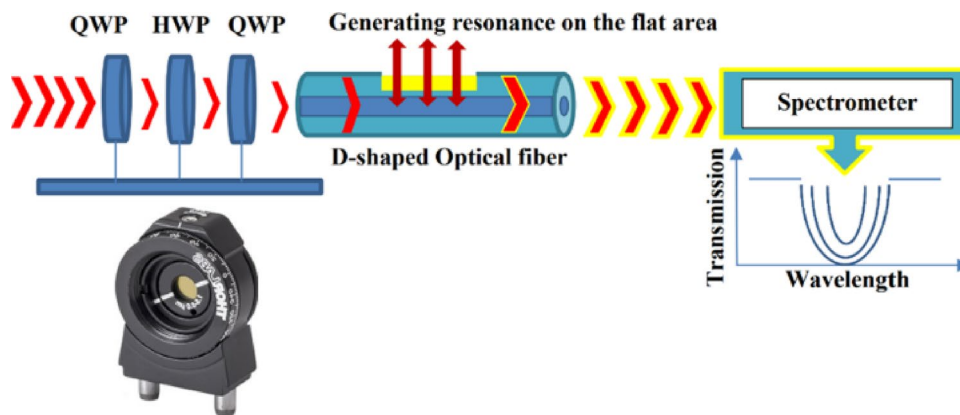


Fig. 3 SPR signal at different deposition times of Au layer

The thickness of the gold layer is optimized by measuring the SPR signal when the D-shaped fiber is exposed to water [19]. The experimental results of the Au-deposited on the D-shaped fiber are depicted in Fig. 3. The gold layer deposition time was within the range of 63–83 s, and the SPR resonance wavelength dip for a 73-s deposition was approximately 500 nm. On the contrary, the resonance wavelength dip for other deposition times is approximately 600 nm. Another parameter that determines the SPR signal's quality is the resonance's width. The relatively narrow width occurs at deposition times of 78 and 83 s. Finally, a deposition time of 78 s was selected as the optimum one for this work. The deposited Au layer (with a deposition time of 78 s) was utilized to fabricate all sensors in this experimental work.

As shown in the scanning electron microscopy (SEM) image, (Fig. 4), the transverse flat surface has a width ranging between 49.3 μm and 50.3 μm . The gold layer was attached to the top of the flat surface, and the depth of the flat surface with gold is still away from the core by 10.92 μm . This finding indicates that the evanescent wave energy is transferred to the surface, leading to solid coupling efficiency because most of the evanescent waves are coupled to the gold/air interface when SPR occurs [20].

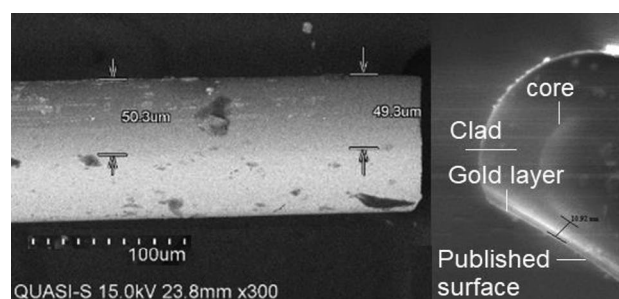


Fig. 4 SEM image of the D-shaped fiber

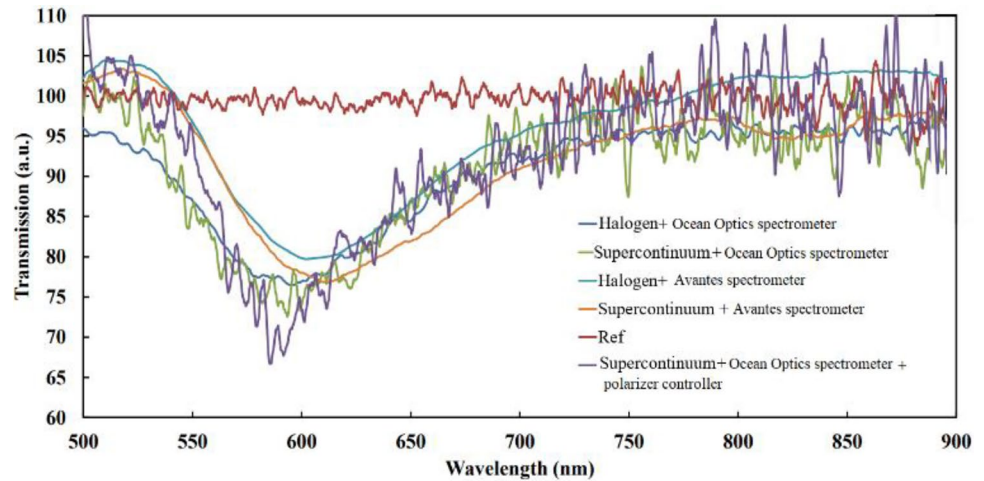
Results and discussion

Light source types

Various light sources show different transmission behaviors related to combining the light source and the spectrometer. The plasmonic behavior depends directly on the spectral location of the plasmonic dip. The transmission of this experiment's light sources and spectrometers has different stability and minimum transmission: purple = 66 a.u., green = 73 a.u., blue = 75 a.u., orange = 76 a.u., and light blue = 80 a.u.; the full width half minimum (FWHM) values are purple = 50 nm, green = 98 nm, blue = 100 nm, orange = 110 nm, and light blue = 115 nm.

Halogen lamp and supercontinuum laser sources were used to excite SPR on D-shaped optical fiber. The orange transmission curve (supercontinuum laser source + Avantes spectrometer) is more stable than the others (light source + spectrometers). In a supercontinuum light source, coherence and polarization deteriorated with increasing pump power [20], as shown by the purple line in Fig. 5, where Ocean Optics spectrometer was used and compared with the Avantes spectrometer (high stability). If the stability is canceled, then the transmission depth and FWHM are the best results using a polarizer controller.

Fig. 5 Plasmonic minimum dip using a different light source and optical spectrometer (17 mm polished length)



The light propagation and coupled conditions in optical fiber are based on the multiple reflections of light inside the fiber. The decay of the transmitted electric field is formed at the interface between the external environment and the fiber optic probe. This transmitted field includes evanescent waves that can easily be affected by the environment’s refractive index variation. Multi-modes can propagate, and each mode has different evanescent waves. Higher-order modes are proportional to optical power distribution in the evanescent region. Mode number is defined as V-number $= \left(\frac{2\pi r}{\lambda} \sqrt{n_{\text{core}} - n_{\text{cladding}}} \right)$, where r is the core radius of the optical fiber. In the D-shaped optical fiber and due to the removal of some cladding, the V-number is $V_d = V_{ef} = \frac{2\pi r_{ef}(d)}{\lambda} \sqrt{n_{\text{core}} - n_{\text{cladding}}}$, where r_{ef} is the effective radius depth of the D-shaped optical fiber. The V-number changes according to the surrounding environment variation. Selecting an excitation light source is crucial to gain a constant power source reflecting their high quantum efficiency, accuracy, and repeatability. The primary effect of quantum efficiency cannot predict the phase shift, which can cause errors in the measurements.

Polarization controller effect

The study was initiated by observing the tuning of the width and dip of the transmission plasmonic curve by using free-space polarization controller. The first experiment consisted of a supercontinuum source connected to the D-shaped fiber sensor through a polarizer controller in a water environment. In this experiment, only one-half wave plate HWP was applied in the polarizer controller bench. The angle of polarization was varied by rotating the HWP. The experimental results of the SPR signal are illustrated in Fig. 6. The deepest resonance dip occurs at 45° HWP and the shallowest resonance dip at 0° HWP. The resonance wavelength slightly shifted from 598.73 to 611.2 nm and from 0° to

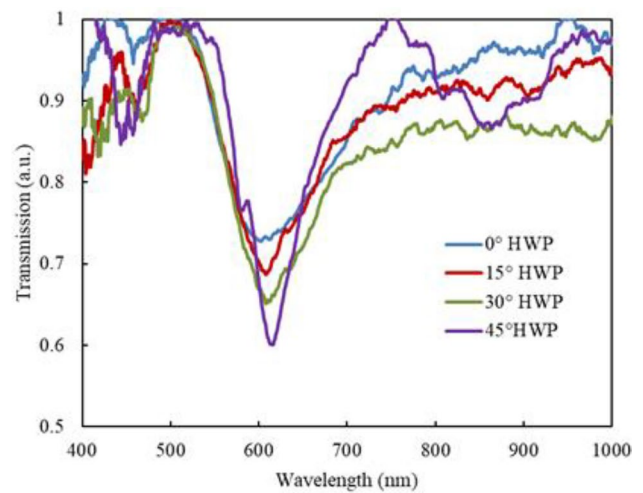


Fig. 6 Effect of angle rotation of the HWP (17 mm polished length)

45° HWP. When the angle induced was more than 45°, the reverse effect was observed, in which the SPR signal behaved reversely. At 90° HWP, the same SPR signal at 0° was re-recorded. Therefore, the angle of HWP is limited between 0° and 45°.

Figure 7 depicts the SPR curves for single and dual waveplates attached to the optical fiber bench and connected to the D-shaped optical fiber with a polished length of 17 mm, coated with gold, and immersed in DI water. Two waveplates were applied to increase the coupling efficiency, and the amount of power emitted from an optical source can be coupled into a gold surface of D-shaped optical fiber. The single D-shaped optical fiber was measured at p-polarized light using HWP only. The result shows that the absorption curve becomes wider with the more profound transmission achieved by connecting the second QWP. The minimum SPR dip for a single optical fiber is 540nm and 800 nm for both designs.

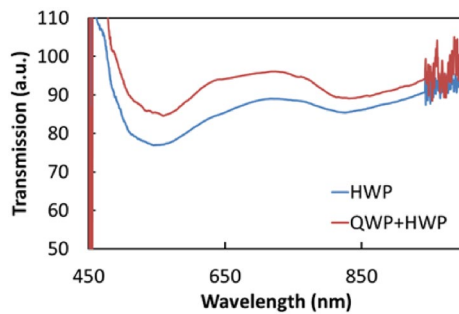


Fig. 7 SPR transmission curve HWP and QWP (17 mm polished length)

Figure 8 shows the sensor design; a single QWP is only used and set initially at 0° , then 45° , and finally at 90° . The sensing area was coated with a gold layer, and the sensing part (25 mm polished length) was immersed in DI water. The D-shaped optical fiber sensor provides an extremely wide SPR dip. This dip ranges between 600 and 950 nm, and two minimum resonance dips at 610 and 790 nm. The broad plasmonic dip typically obtains inaccurate results [21]. Based on the results, it has been determined that a polished length of 25 mm is not suitable for plasmonic sensors. Therefore, the research will continue with a polished length of only 17 mm.

Figure 9 shows the sensing signal using three waveplates for polarization variation. The sensing signal is an output signal variation, such as a transmittance signal based on the attached analyte. The first QWP is set to 45° , 90° , and 0° . The supercontinuum laser source illuminated the D-shaped optical fiber and was received by a spectrometer (Avantes). The effect appears as a variation in the dip and width of the SPR curve. Dip variation distinguishes s-polarization from p-polarization. The p-polarization appeared as a relatively deep dip when the first QWP was set at 90° . The evanescent waves could only be strong at p-polarization [19]. This evanescent wave causes a variation in direction at each reflection belonging to the electric field vector. The s and p polarization are due to the decomposition of the plane of

incidence of the electric field vector; the plane of incidence is perpendicular to the direction of propagation. This experiment indicates sensitivity because, according to the literature, p-polarization has higher sensitivity than s-polarization [19]. The results also show two dips, 630 and 740 nm, and the deepest transmission SPR curve was at $90^\circ.0^\circ.45^\circ$. This setup type will help in sensor applications, such as evaluating the desorption and absorption of a coated layer for subsequent experiments. To test sensors and other optical devices, it is very important to use a polarizer controller that can measure how these devices respond to different light polarizations.

Evaluation of temperature effect

The precision of results is advantageous in optical fiber sensors and has a very rapid response [22]. Figure 10a shows the temperature effect on the SPR plasmonic curve, transmission variation, and wavelength by using the stage polarizer at the $90^\circ.0^\circ.45^\circ$ fiber-based SPR (17 mm polished length). The wavelength shift and stability indicate the best performance as a temperature sensor using QWP-HWP-QWP. Figure 10b shows that the optical fiber results were obtained without the stage polarizer. It appears that the sensor's stability can be enhanced under temperature changes when compared to the D-shaped optical fiber sensor design with a stage polarizer. The sensor's sensitivity measures 0.2 nm/degree with the stage polarizer and 0.3 nm/degree without at 40°C .

Refractive index sensor

The sensing test for 17 mm D-shaped optical fiber with and without waveplates at 40°C is shown in Fig. 11 using standard refractive index Series AAA (Cargille Laboratory). The results show an apparent shift (Fig. 11a) in the wavelength and transmission power compared to the waveplate sensor design of $90^\circ.0^\circ.45^\circ$ (Fig. 11b), which has a recognizable transmission power shift. The transmission power shift becomes more evident with waveplates than without waveplates. The sensor's behavior showed a resonance dip

Fig. 8 Single QWP-coated gold

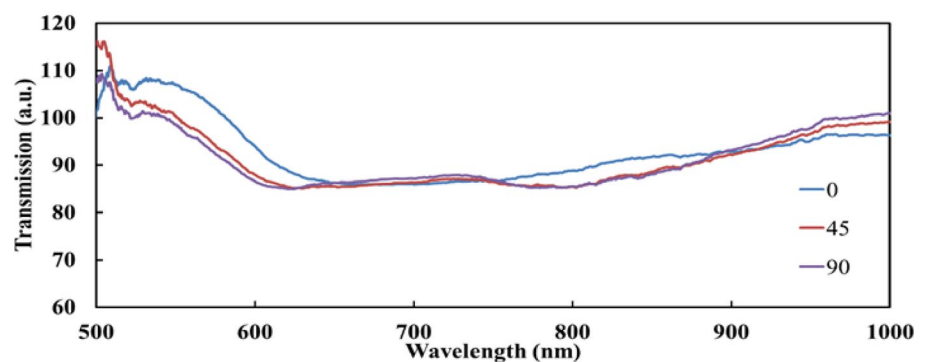


Fig. 9 Transmission curves of the plasmonic effect at different waveplate angles (25 mm polished length)

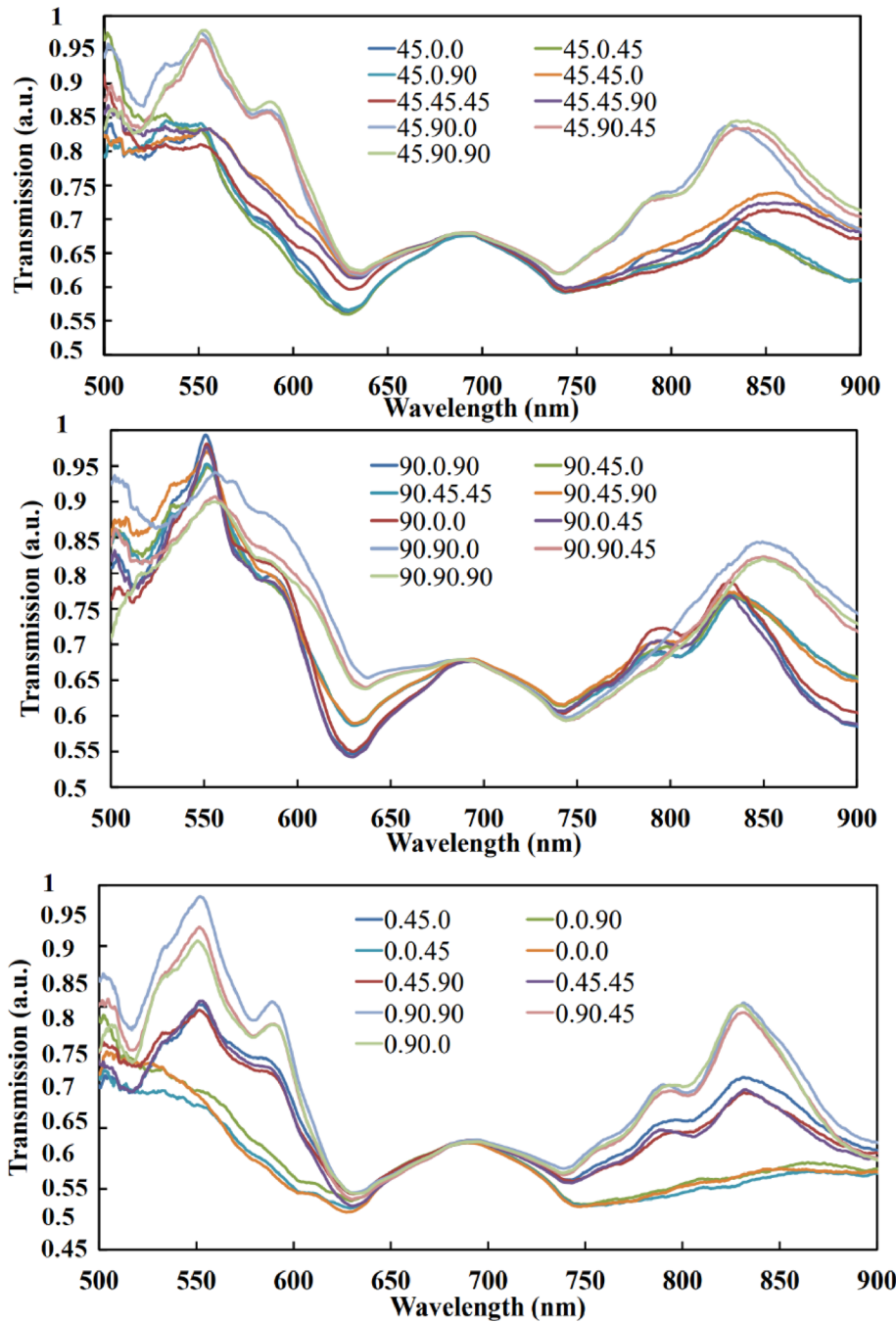


Fig. 10 Effect of temperature on the plasmonic dip: **a** with stage polarizer and **b** without stage polarizer

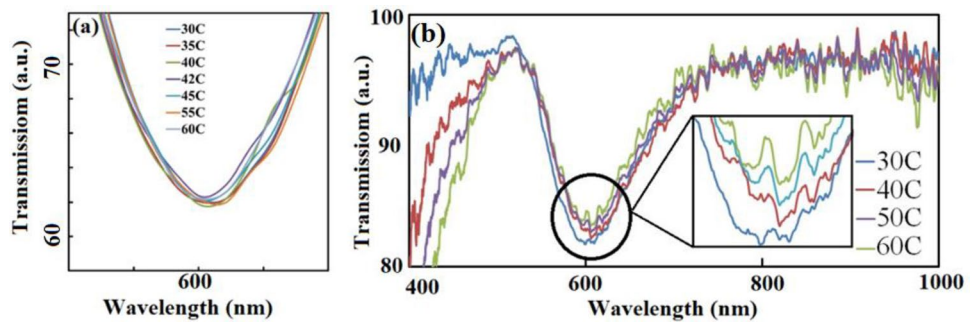


Fig. 11 SPR transmission curves **a** without stage polarizer and **b** with stage polarizer

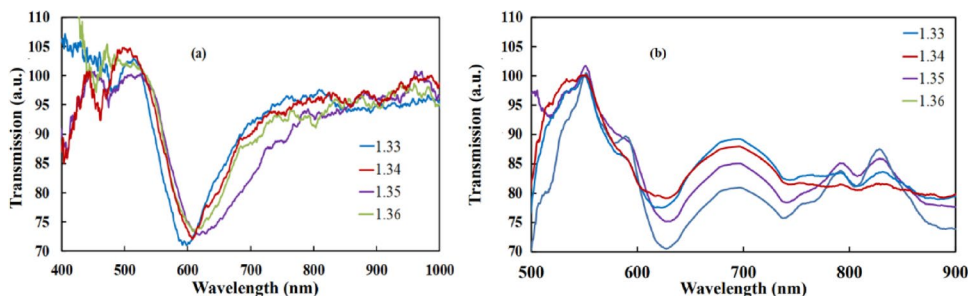
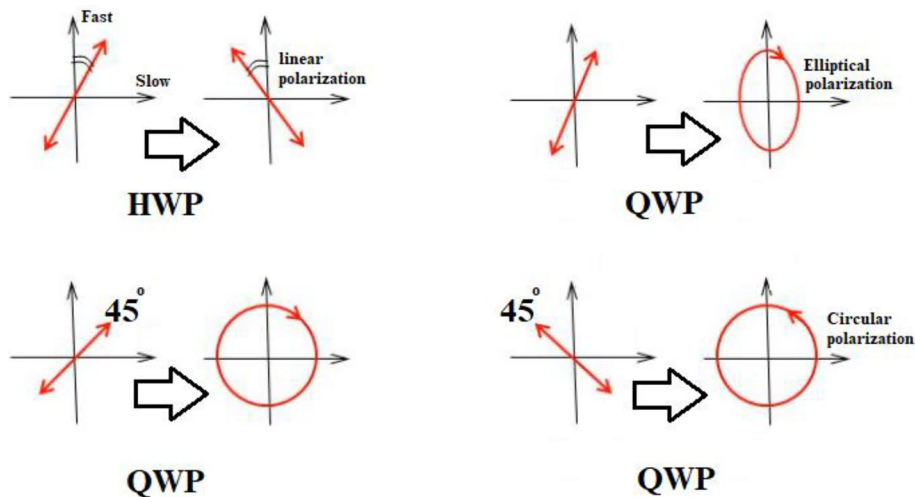


Fig. 12 Polarized light variation before input inside the optical fiber



when the waveplates were attached to the sensor system. Using the waveplate reduces the transmission magnitude by 20% due to canceling some light components and allows the polarized light to pass and be coupled to the plasmonic surface, thereby increasing the accuracy of the resonance dip and reducing the sensitivity when only P-polarized light is allowed in the plane. The polarization state plays a crucial role in the optical power of the transmission. Therefore, the sensor characteristics can be modified by exploiting the polarization [21].

The beam of light consists of two electric field components. The amplitude of these components varies as a function of frequency. Unpolarized light becomes polarized when both components vary in phase and amplitude through the first QWP. The changes in output polarization in terms of coupling mode in polarization occur because of birefringence modifications that serve as perturbations along with the fiber. Birefringence is normally induced because of the fiber bending and some stress induced by polishing processes [23].

The first waveplate converts light into a linear polarization. Linear polarization is associated directly with phase retardation f and s , which are fast and slow azimuths, respectively. The polarizer configuration is HWP sandwiched between both QWPs, and the plates can always freely spin

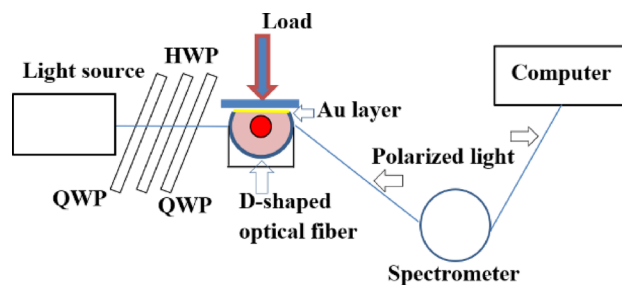


Fig. 13 Polarization-based D-shaped fiber sensor

around the optical path. HWP rotates the linear polarization state to any angle; thus, any desired polarization state is translated by the last QWP, as shown in Fig. 12.

Photoelastic effect sensor

Any external stress causes changes in the polarization state [24]. The external perturbation can be detected using a D-shaped optical fiber as a sensor for the photoelastic effect. Figure 13 shows the polarization-based D-shaped optical fiber sensor connected between the light source and spectrometer (supercontinuum laser and Avantes spectrometer). The sensing area (17 mm polished length)

was coated with a gold layer to enhance the plasmonic optical response. The waveplate sensor design was set to $90^{\circ}.0^{\circ}.45^{\circ}$. The load was applied in a range of grams to prevent cutting fiber. The loads are 10 and 15 g applied in sequence. The D-shaped optical fiber is placed in a pocket slot of the metal chamber and covered by a thin plastic surface.

The sensing results were recognized when two different loads were applied to the D-shaped optical fiber. The resonance wavelength at load = 0 was 612.37, and the transmission power = 0.618 (a.u.) (Fig. 14). The maximum sensitivity was 1.05 nm/g at 5 g weight. The change in the physical property due to the applied weight causes fiber perturbation, which leads to optical path variation. The effect of these parameters is a variation in optical wave propagation inside the sensing area. Finally, the transmission power changes horizontally and vertically. Usually, the reduction in intensity is caused by bending the optical fiber and losing the light intensity in the cladding [25]. The polarization state of light inside the optical fiber is a sensitive property whose change can be found directly by the transmission signal. The wavelength shift result depends on the output polarization; this wavelength change is normally related to the dispersion of propagation constants of the mode excited [26].

A particular Hg ion in DI water was used to measure the plasmonic response (transmitted power shift) and recorded at fixed time intervals measured every 10 s. This test was built using three waveplate design (supercontinuum laser and Avantes spectrometer), 17 mm polished length, $90^{\circ}.0^{\circ}.45^{\circ}$, and $\sim 40^{\circ}\text{C}$ experiment temperature. rGO/ γ - Fe_2O_3 and PVC (polyvinyl chloride) are powders dissolved in ethanol, then mixed and sprayed on the Au layer to form the rGO/ γ - Fe_2O_3 /PVC sensing layer. The SPR stability test was conducted for 15 ppm concentrations. Figure 15 depicts the sensor results of practical tests with waveplates for stability. Stability was confirmed for rGO/ γ - Fe_2O_3 /PVC. The results also show wavelength shift and intensity shift. The wavelength shift was equal to 590 Pico between DI water and 15 ppm Hg ions. Repeating the test shows non sequitur arranged in intensity shift, but interestingly, no change was detected in the more crucial wavelength shift. However, the intensity shift varies in the range of 0.172 a.u. of the transmission power. The shift in the transmission power may be due to the liquid temperature that increases the circulation of heavy metals in liquid, increasing the number of Hg ions attached to the sensing area.

Different concentrations of Hg ions were tested using the same previous fiber design (supercontinuum laser and

Fig. 14 SPR transmission curve under the effect of load sensing stability and performance

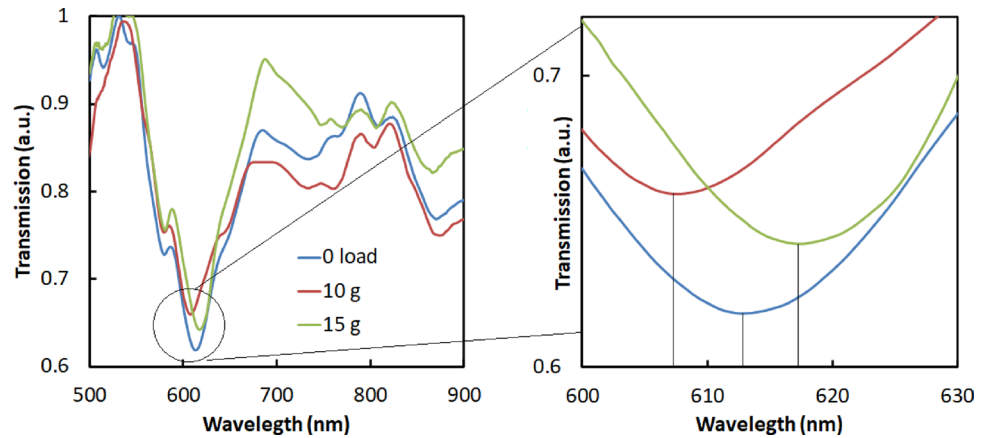
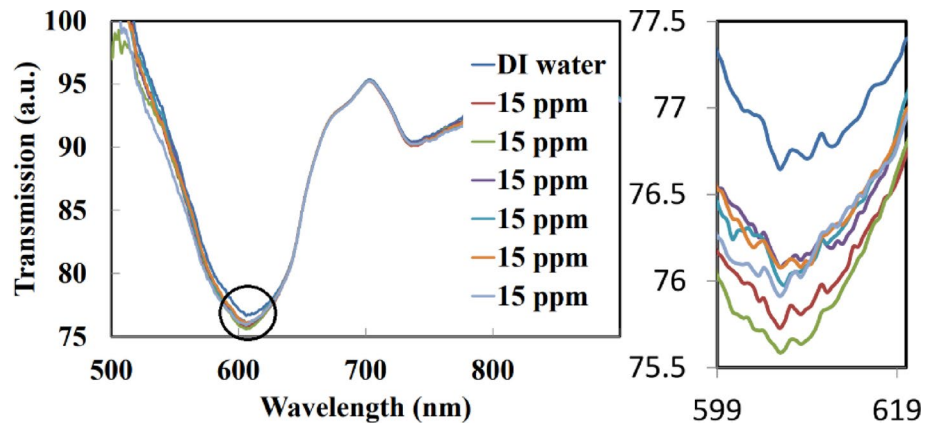


Fig. 15 SPR transmission curve stability at constant Hg concentration



Avantes spectrometer), 17 mm polished length, $90^{\circ}.0^{\circ}.45^{\circ}$, and $\sim 40^{\circ}\text{C}$. The sensor shows an unsequenced shift based on the used Hg ion concentrations. The effect of temperature can play a vital role in increasing sensitivity but, at the same time, does not provide sequence shifts according to the concentration value. This test was performed for 180 s for each concentration to allow the optical signal to take the final minimum position (Fig. 16).

The response and rise time were tested, as shown in Fig. 17. This test measured the response and rise time according to the Hg^{2+} concentrations. The response time and rise time have an average of 80 s for Hg^{2+} concentrations (15, 25, and 35 ppm). The response time describes the speed of the Hg^{2+} reaction to change the surface during actual work. This test is essential to compare the relative performance of various sensor types or analyze the diversity with a production batch.

When precise control is required, the reaction time is essential. When an instrument's feedback signal controls a system, the controller cannot respond to changes that occur faster than the speed of this instrument's reaction. Therefore, quick and temporary changes are unnoticed, or the measurement instrument inaccurately controls the system in response. In the worst-case scenario, the measurement instrument's lag with firmly tuned controllers may result in unnecessary fluctuation or lengthening of the stabilization time. As a general guideline, an instrument's response time is adequate when it is approximately half that of the system's controlled shortest-time constant.

The selectivity coefficients of this type of sensor are based on the chemical characteristics of heavy metals to be detected. Hg^{2+} is possibly produced by dissolving the mercury elements in oxidizing acids. Mercury's atomic weight and atomic number are 200.6 and 80, respectively. Mercury

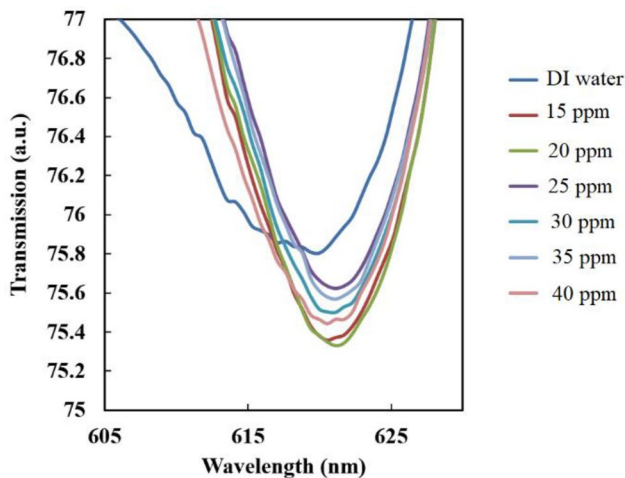


Fig. 16 Power of the transmission for SPR dip under the effect of Hg ion at different concentration values and at 40°C

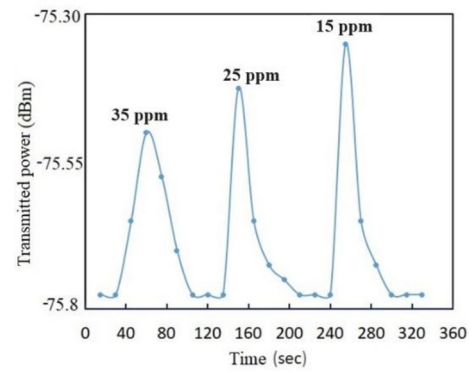


Fig. 17 Rise time and response time for Hg^{2+}

is close to Lead, with atomic weight and atomic number of 208 and 82, respectively. Detecting these heavy metals in the same liquids, especially at low concentrations, requires a precise design [27, 28]. Figure 18 shows the selectivity test for different heavy metals (Hg^{2+} , Cd^{2+} , Pb^{2+} , and Cu^{2+}) using 15 ppm for all concentrations. The result shows various shifts by using other heavy metals. However, the most significant change was recognized for Hg ions.

Conclusion

This research discusses the performance of the D-shaped optical fiber-based SPR in different conditions. The evaluation begins with optimizing Au deposition onto the D-shaped fiber, where the optimum deposition time is 78 s. The polarization effect on the sensor was also investigated using a polarizer controller. The shallowest resonance

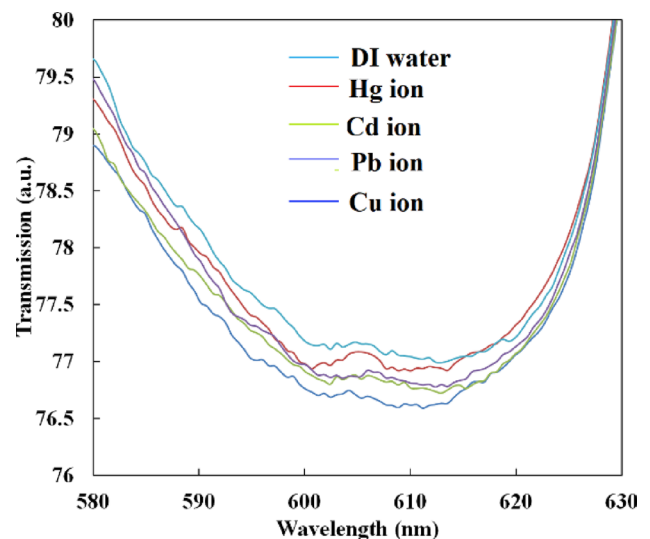


Fig. 18 Sensor selectivity at different heavy metals

response was found to occur when the HWP was set to 0° , while the most profound resonance response was observed when the HWP was changed to 45° . The temperature effects were found as negative shifts in absorption for fiber-based SPR using a polarizer controller compared with that without a polarizer controller ranging from 30 to 60 °C. This shift indicates the best performance as a temperature sensor. The sensor shows substantial variation in the photoelastic effect according to the applied load with a maximum sensitivity of 1.05 nm/g at 5 g weight. For higher stability at constant Hg ion concentrations, the fiber-based SPR is a suitable option. This study proves that the best length for D-shaped optical fiber for the plasmonic sensor is no longer than 17 mm. It can be difficult to identify the shift in the plasmonic dip due to its broad nature in the 25 mm sample. The sensing layer of rGO/ γ -Fe₂O₃/PVC possibly works as Hg ion sensor for high stability and good response time at 40 °C.

Acknowledgements This work has been supported by Universiti Putra Malaysia (UPM) through the engineering department. The authors thank professors for their valuable help with the sample preparation and test.

Data availability Data underlying the results presented in this paper are not publicly available at this time but may be obtained from the authors upon reasonable request.

Declarations

Conflict of interest The authors declare no conflicts of interest.

References

- M.A. Fakhri, E.T. Salim, S.M. Tariq, R.K. Ibrahim, F.H. Alsultany, A. Ali, S.F. Alwahib, H. Alhasan, S.C.B. Gopinath, Z.T. Salim, U. Hashim, A gold nanoparticles coated unclad single mode fiber-optic sensor based on localized surface plasmon resonance. *Sci. Rep.* **13**(1), 5680 (2023)
- G. Xiao, W. J. Bock, Photonic sensing: principles and applications for safety and security monitoring, p336, (2012)
- B.P.N. Jennifer, M. Brockman, R.M. Corn, Surface plasmon resonance imaging measurements of ultra thin organic films. *Annu. Rev. Phys. Chem.. Rev. Phys. Chem.* **51**(October), 41–63 (2000)
- Y. Liu, W. Yu, Strong intensity modulation of surface plasmon polaritons by a dielectric layer. *IEEE Photonics Technol. Lett.* **24**(24), 2214–2217 (2012)
- A.A. Kruchinin, Y.G. Vlasov, Surface plasmon resonance monitoring by means of polarization state measurement in reflected light as the basis of a DNA-probe biosensor. *Sens. Actuators B Chem.* **30**(1), 77–80 (1996)
- Y. Su et al., Surface-plasmon-resonance-based optical fiber curvature sensor with temperature compensation by means of dual modulation method. *Sensors (Switzerland)* **18**(8), 1–12 (2018)
- H.P. Chiang et al., Surface plasmon resonance monitoring of temperature via phase measurement. *Opt. Commun.* **241**(4–6), 409–418 (2004)
- M. Ghorbanpour, C. Falamaki, A novel method for the production of highly adherent Au layers on glass substrates used in surface plasmon resonance analysis: substitution of Cr or Ti intermediate. *J. Nanostruct. Chem* **3**, 1–7 (2013)
- J. Frischeisen, N. Reinke, C. Ostermayr, J. Neumann, and S. Nowy, Surface plasmon resonance sensor based on a planar polychromatic OLED light source. In: *Proceeding of SPIE*, 7003, (2008).
- H.P. Ho, S.Y. Wu, M. Yang, A.C. Cheung, Application of white light-emitting diode to surface plasmon resonance sensors. *Sens. Actuators B Chem.* **80**(2), 89–94 (2001)
- H. Yan and G. Lai-xu, Realization of surface plasmon resonance sensor based on wavelength modulation by using 50 nm broadband light source*. *IEEE*, pp. 182–185, (2010).
- R. Chlebus, J. Chylek, D. Ciprian, P. Hlubina, Surface plasmon resonance based measurement of the dielectric function of a thin metal film. *Sensors (Switzerland)* **18**(11), 8–19 (2018)
- J.H. Ahn, T.Y. Seong, W.M. Kim, T.S. Lee, I. Kim, K. Lee, Fiber-optic waveguide coupled surface plasmon resonance sensor. *Opt. Soc. Am.* **20**(19), 633–642 (2012)
- A. Abdulkhaleq Alwahib, S. Fawzi Alhasan, M.H. Yaacob, H.N. Lim, M. Adzir Mahdi, Surface plasmon resonance sensor based on D-shaped optical fiber using fiberbench rotating wave plate for sensing pb ions". *Optik (Stuttg)* **202**, 163724 (2020)
- H.D. Abdulkareem, A.A. Alwahib, B.R. Mahdi, PCF-multimode/endsless fiber sensor for respiratory rate monitoring. *Optoelectron. Lett.* **19**(1), 8–13 (2023)
- P. Photonics, D Shaped / Side-polished optical fibers. http://www.phoenixphotonics.com/website/technology/documents/DShapedSidePolishedFibersV2_01405.pdf
- A.A. Melo, M.F.S. Santiago, T.B. Silva, C.S. Moreira, R.M.S. Cruz, Investigation of a D-shaped optical fiber sensor with graphene overlay. *IFAC-PapersOnLine* **51**(27), 309–314 (2018)
- R. Verma, B.D. Gupta, Detection of heavy metal ions in contaminated water by surface plasmon resonance based optical fibre sensor using conducting polymer and chitosan. *Food Chem.* **166**(6), 568–575 (2015)
- C.B. Brennan, L. Sun, S.G. Weber, Investigations of prussian blue using surface plasmon resonance. *Sens. Actuators B Chem.* **72**, 1–10 (2001)
- X. Yu et al., An efficient approach for investigating surface plasmon resonance in asymmetric optical fibers based on birefringence analysis. *Opt. Express* **18**(17), 17950–17957 (2010)
- F.H. Suhailin, A.A. Alwahib, Y.M. Kamil, M.H. Abu Bakar, N.M. Huang, M.A. Mahdi, Fiber-based surface plasmon resonance sensor for lead Ion detection in aqueous solution. *Plasmonics* **15**, 1369–1376 (2020)
- J. F. Algorri and V. Urruchi, Temperature sensor based on a liquid crystal plasmonic wire grating. In *IEEE Sensors Proceedings*, 16–19, (2014).
- K. Arun, S. Pilevar, Measurements on variation of birefringence with depth of polishing in elliptic core fibers. *Opt. Commun.* **72**(3), 187–189 (1989)
- P. Khandelwal, Optical fiber sensors: classification & applications. *Int. J. Latest Technol. Manag. Appl. Sci.* **II**(vii), 22–25 (2013)
- J. Jena, S. Wassin, L. Bezuidenhout, M. Doucouré, T. Gibbon, Polarization-based optical fiber acoustic sensor for geological applications. *J. Opt. Soc. Am. B* **37**(11), A147 (2020)
- V.V.G.K. Inavalli, V. Pottapinjara, N.K. Viswanathan, Wavelength dependence of the polarization singularities in a two-mode optical fiber. *Int. J. Opt.* (2012). <https://doi.org/10.1155/2012/358093>
- S. Menon, S.P. Usha, H. Manoharan, P.V.N. Kishore, V.V.R. Sai, Metal-organic framework-based fiber optic sensor for chromium(VI) detection. *ACS Sens.* **8**(2), 684–693 (2023)

28. J. Jumal, B.M. Yamin, M. Ahmad, L.Y. Heng, Mercury ion-selective electrode with self-plasticizing Poly(*n*-butylacrylate) membrane based on 1,2-Bis-(*N*⁺-benzoylthioureido)cyclohexane as ionophore. *APCBEE Proc.* **3**, 116–123 (2012)

Springer Nature or its licensor (e.g. a society or other partner) holds exclusive rights to this article under a publishing agreement with the author(s) or other rightsholder(s); author self-archiving of the accepted manuscript version of this article is solely governed by the terms of such publishing agreement and applicable law.

Publisher's Note Springer Nature remains neutral with regard to jurisdictional claims in published maps and institutional affiliations.